International Journal of Mechanical and Production Engineering Research and Development (IJMPERD)
ISSN(P): 2249-6890; ISSN(E): 2249-8001
Vol. 9, Issue 4, Aug 2019, 219-228

BUCKLING OF CONES WITH IMPERFECT LENGTH SUBJECTED TO AXIAL COMPRESSION

O. IFAYEFUNMI, F. M. MAHIDAN & S. H. WANG

Fakulti Teknologi Kejuruteraan Mekanikal dan Pembuatan,

Universiti Teknikal Malaysia Melaka, Malaysia

ABSTRACT

The paper considers the effect of imperfect length on the buckling behavior of mild steel truncated cone subjected to axial compression. The contact interaction problem between the rigid plate and the cone was successfully benchmarked against experimental data on axially compressed cone with imperfection amplitude-to-thickness ratio, A/t = 0.28 and 5.6. Conical shells are assumed to be made from mild steel with the following geometric properties: big radius-to-small radius ratio, r2/r1 = 2.0; small radius-to-thickness ratio, r1/t = 25; axial length-to-big radius ratio, L/r2 = 2.24; nominal wall thickness, t = 1 mm and cone angle, β = 12.6°. A total of fifteen (15) mild steel cones were collapsed by axial compression. Ten samples with A/t of 0.28 and another five samples with A/t of 5.6. Experimental and numerical load carrying capacity for imperfect cones were obtained for both cases above. The results indicate that imperfection amplitude strongly affect the buckling strength of conical shells. In addition, it was observed that as the magnitude of imperfect length to wall thickness increases, the contact interaction between the cone and the rigid plate changes. Finally, the effect of number of waves on buckling load of cones under axial compression is less significant.

KEYWORDS: Buckling, Imperfect Cone, Axial Compression, Mild Steel & ABAQUS

Received: Apr 26, 2019; **Accepted:** May 15, 2019; **Published:** Jun 21, 2019; **Paper Id.:** IJMPERDAUG201923

Original Article

INTRODUCTION

Thin-walled conical shells are commonly used for offshore and pipeline applications. Typical applications include: (i) transition element between two cylinders of different diameter, (ii) piles for holding jackets when driven into the seabed, and (iii) legs of offshore drilling rigs. When used for such applications, the contact interaction between two neighboring shell structures becomes very important – since the safe performance of such structures are generally believed to be sensitive to imperfection such as initial geometric imperfection, imperfect length, imperfect boundary condition, crack/material discontinuity etc. [1]. However, the degree of sensitivity of conical shell structures to imperfection is said to be strongly dependent on its geometric parameter [2]. Review of past literatures on the imperfection sensitivity of conical shells can be found in [3, 4].

Several investigations have been conducted on the imperfection sensitivity of conical shell structures. Although, the most widely considered a form of imperfection are the initial geometric imperfection. References into the influence of initial geometric imperfection (i.e., eigenmode shape imperfection, axisymmetric outward bulge, localized smooth dimple and simple perturbation load) on the load carrying capacity of conical shells can be found in [5 - 12]. Moreover, few studies have been devoted to other forms of imperfections such as imperfect boundary condition [13 – 17], crack/material discontinuity [18 - 20]. Surprisingly, it is evident from literature survey, that there has been no information of the imperfection sensitivity of conical shells having uneven axial

length. The only available information is on imperfect cylinder having uneven axial length, [21, 22]. Hence, a question on the role of imperfect length on the buckling behavior of conical shells is a valid one.

The current paper examines the imperfection sensitivity of truncated mild steel cone having uneven length subjected to axial compression. The effect of (i) increasing the number of waves, and (ii) contact interaction problem by increasing the axial imperfection amplitude to thickness ratio, A/t, on the buckling load of axially compressed conical shell is presented. This is both experimental and numerical approaches. Numerical analysis is based on the ABAQUS FE code, Ref. [23].

MATERIAL AND METHODS

Specimens Manufacturing and Material

Ten laboratory scale imperfect conical shells were manufactured from 1 mm mild steel plate and tested under axial compression. The geometric parameters of the specimens were assumed to be: big radius-to-small radius ratio, r2/r1 = 2.0; small radius-to-thickness ratio, r1/t = 25; axial length-to-big radius ratio, L/r2 = 2.24; nominal wall thickness, t = 1 mm and cone angle, β = 12.6°. The cones have imperfection amplitude-to-thickness ratio, A/t = 0.28.

To manufacture the specimens, several steps were followed. First of all, the samples were cut out to the desired dimension of the flat plate using a laser cutting machine. Then, the cut out samples are rolled to conical shape using the conventional rolling machine. After the rolling process, the seam between the two neighbouring meridional free edges of the cone are welded together using Metal Inert Gas (MIG) welding process. During the manufacturing process, initial geometric imperfection having sinusoidal wave along the compressed edge of the imperfect cones were introduced as depicted in Figure 1. The choice of introducing uneven length at the small radius end of the cone can be attributed to the fact that for conical shells the spread of plastic strain is concentrated within the small radius end of the cone [24, 25]. The number of waves, (N = 0, 4, 6, 8, 10 and 12). All cones were manufactured in pairs except for N = 6 and 10.

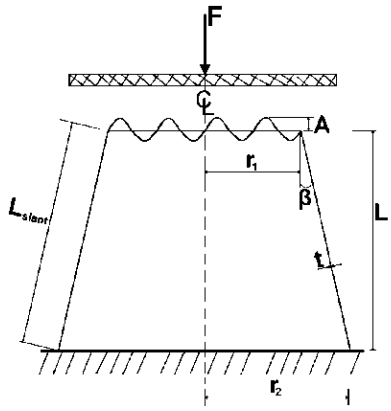

Figure 1: Geometry of the Analyzed Cone Having Sinusoidal Non-Uniform Length with Number of Waves, N = 4

Next, six flat tensile coupons (three in the axial direction - V1, V2, V3 and another three in the lateral direction - H1, H2, H3) were cut from the same material from which the conical model are made. The design of the tensile coupon is according to British standards, [26]. All tensile specimens were tested until they fail using an instron machine at the rate of 1 mm/min. Table 1 presents the material data obtained from the uni-axial tensile test. The Poison's ratio of the material was assumed to be 0.3 (data taken from material data sheet).

Table 1: Set of Material Data Obtained From Uni-Axial Tensile Test

Tensile Coupons	Young's Modulus, E (GPa)	0.2% Offset Yield Stress, σ_{yp} (MPa)	Ultimate Tensile Stress (MPa)
H1	164.050	226.373	319.69
H2	148.864	233.460	326.33
H3	179.815	230.185	325.35
V1	194.938	227.276	324.99
V2	158.520	230.003	328.99
V3	166.559	231.347	330.20
Average	168.791	229.774	325.925

Lastly, to benchmark the contact interaction problem between the rigid plate and the deformable imperfect cone against experimental data. Additional five conical specimen having the same geometry as previously discussed were manufactured from 1mm mild steel plate and tested under axial compression. The cones have imperfection amplitude-to-thickness ratio, A/t = 5.6. Again, the manufacturing technique employed were the same as discuss earlier except for the fact that in this case, the cutting process was carried out using abrasive waterjet machine. And the number of sinusoidal waves, (N = 0, 4, 6, 8 and 10). In a similar fashion, flat tensile coupons were cut from the same material from which the conical model are made and tested until they fail using instron machine at the rate of 1 mm/min. The average material properties obtained were as follows: Young's Modulus E = 212.7GPa, Poisson ratio, $\nu = 0.3$ and the yield stress based on 0.2% offset, σyp = 218 MPa. Two different contact interaction between the rigid plate and the compressed edge of the cone were analyzed, viz: (i) contact interaction with set of top edge nodes and (ii) contact interaction with set of N-point nodes – as sketched for the case of cylinder in [21] (see Figure 12 of [21]).

Specimen Measurement and Testing

Before testing, manufacture-induced imperfections were taken into consideration. A number of measurements (i.e., wall thickness, diameter, axial length and slant length) of all the conical models were taken. Firstly, the wall thickness of the cones was measured at eleven (11) equal points along the axial meridian using micrometer screw gage. This was then repeated along the circumference of the cone at 36° apart, resulting in 11 x 10 = 110 measuring points. The minimum thickness tmin, maximum thickness tmax, average thickness tave and the standard deviation tstd for all the manufactured cones are provided in Table 2. Secondly, the inner and outer diameters of the specimens were measured using digital Vernier caliper. Measurements were taken at five equally spaced diameters at the top and bottom ends respectively. The average measured mid-surface diameter for all specimens are given in Table 2. Thirdly, digital Vernier caliper was used to measure the axial length and slant length of the cones at eleven equal point. The measured average axial length and slant length are also presented in Table 2. These shape measurements were assumed to represent the most obvious characteristic of the specimens. All fifteen conical shells were subjected to axial compressive load using instron machine. Prior to loading, the specimen was covered with top and bottom plate. An incremental load is applied to the cone at the rate of 1 mm/min (the same loading rate employed for the material testing). During the experiment, the axial load and its corresponding compression extension of the cones were recorded using the machine controller. To validate the readings of the compression extension from the machine controller, dial gauge were placed on the moveable platen of the instron as shown in Figure 2.

Table 2 : Measured Wall Thickness, Mid-Surface Diameters at the Top and Bottom Ends ($\overline{2r_1}$ And $\overline{2r_2}$),Average Axial Length ($\overline{L}$) and Average Slant Length ($\overline{L_{slant}}$) of Tested Cones

Model	N	A/t	t_{min}	t_{max}	t_{ave}	$\overline{2r_1}$	$\overline{2r_2}$	$\overline{L}$	$\overline{L_{slant}}$	t_{std}
			(mm)							
CN1	0	0.28	0.950	0.960	0.956	49.709	99.022	112.992	114.766	0.00497
CN2	0	0.28	0.950	0.960	0.955	49.526	98.776	112.712	114.734	0.00500
CN3	4	0.28	0.950	0.990	0.961	49.053	97.667	112.406	114.454	0.00813
CN4	4	0.28	0.950	0.970	0.959	49.681	99.210	112.504	114.645	0.00852
CN5	6	0.28	0.950	0.970	0.955	49.616	98.689	112.690	114.761	0.00565
CN6	8	0.28	0.950	0.970	0.959	49.717	99.047	112.472	114.579	0.00886
CN7	8	0.28	0.950	0.990	0.962	49.520	98.825	112.587	114.591	0.00946
CN8	10	0.28	0.950	0.970	0.956	49.686	98.863	112.586	114.756	0.00598
CN9	12	0.28	0.950	1.010	0.955	50.008	98.876	112.818	114.737	0.00818
CN10	12	0.28	0.950	1.080	0.957	49.392	98.758	112.796	114.755	0.01434
CN11	0	5.6	0.980	1.000	0.988	50.550	99.728	113.16	115.40	0.00406
CN12	4	5.6	0.985	0.995	0.991	50.084	99.886	113.25	115.34	0.00394
CN13	6	5.6	0.980	1.000	0.990	50.499	99.615	113.22	115.35	0.00446
CN14	8	5.6	0.980	1.000	0.990	51.107	100.062	113,28	115.32	0.00493
CN15	10	5.6	0.980	1.005	0.988	51.581	99.922	113.27	115.28	0.00443

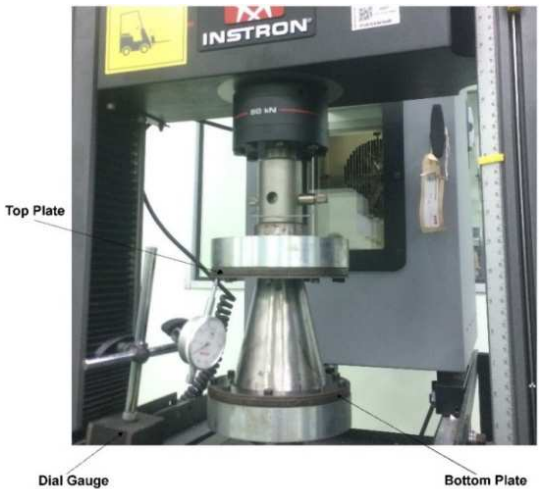

Figure 2: Photograph of the Test Arrangement for Cone (CN1) Subjected to Axial Compression.

RESULTS AND DISCUSSIONS

Experimental results for fifteen axially compressed perfect and imperfect conical models subjected to axial compression are given in Table 3. It can be seen from Table 3, that the collapse load of the perfect cones reduces with the introduction of non-uniform length. In addition, four pairs of nominally identical cones failed with similar collapse load. The errors in collapse load within each pair were: 2% (CN1 vs CN2), 4% (CN3 Vs CN4), 2% (CN6 vs CN7), and 3% ((CN9 vs CN10). Hence, confirming repeatability of experimental data. Again, it is obvious that increasing the wave number on the cone, results in minimal influence on the collapse load of the cone. Therefore, it can be said that increasing the waves number has a secondary effect on the collapse load of the cone. This is true for the case of cylindrical shells reported in [22].

Table 3: Comparison of Experimental and Numerical Buckling Load of Imperfect Cones with Different Wave Number and Different Imperfection Amplitude. Note: Contact Interaction (CN1 – CN10 = Set of Top Edge Nodes; CN11 – CN15 = Set of N-Point Nodes)

Model	N	A/t	Buckling Load of Cone (kN)		% Difference
			Exptl	ABAQUS	
CN1	0	0.28	38.99	38.24	1.9
CN2	0	0.28	39.91	38.21	4.3
CN3	4	0.28	37.41	36.41	2.7
CN4	4	0.28	39.06	36.33	7.0
CN5	6	0.28	38.86	34.53	11.1
CN6	8	0.28	34.71	34.39	0.9
CN7	8	0.28	33.96	34.51	1.6
CN8	10	0.28	35.79	34.71	3.0
CN9	12	0.28	37.47	34.48	8.0
CN10	12	0.28	36.40	34.55	5.1
CN11	0	5.6	32.20	33.46	3.9
CN12	4	5.6	9.51	8.03	15.6
CN13	6	5.6	8.54	8.35	2.2
CN14	8	5.6	9.50	8.79	7.5
CN15	10	5.6	9.85	9.40	4.6

Plot of experimental collapse load against compression extension for two nominally identical perfect cone (CNI and CN2) follow the same collapse paths at the pre-collapse and the post-collapse region – as can be seen in Figure 3. Again, there is very good agreement for both cones in terms of collapse load and the compression extension. A similar plot for imperfect cones with N = 8 is presented in Figure 4. Again the failure paths of both cones was the same.

Validation of experimental data were carried out through numerical simulation using ABAQUS FE code. The numerical predictions employed the use of measured specimen data i.e., average thickness and average mid-surface diameter (see Table 2). Material data obtained from uni-axial test were used in the numerical calculation and the material is modelled as elastic-perfectly plastic. As shown in Figure 1, the cone is assumed to be fixed at the big radius ends, while the same condition was employed at the top ends except movement in the axial direction. Conical specimens were modelled as deformable body using four noded shell elements with six degree of freedom (S4R). Axial load was applied to the small radius end of the cone through a horizontal and rigid plate moving downward (see Figure 1). To apply the axial load, a reference node was defined at the center of the rigid plate. During the computation, surface-to-surface contact interaction between the rigid plate and the cone using master-slave algorithm was employed. In the master-slave algorithm, the rigid plate is referred to as the master, while the set of all nodes at the top edge of the cone is referred to as the slave. Then, non-linear static RIKS analysis was carried out on the conical model.

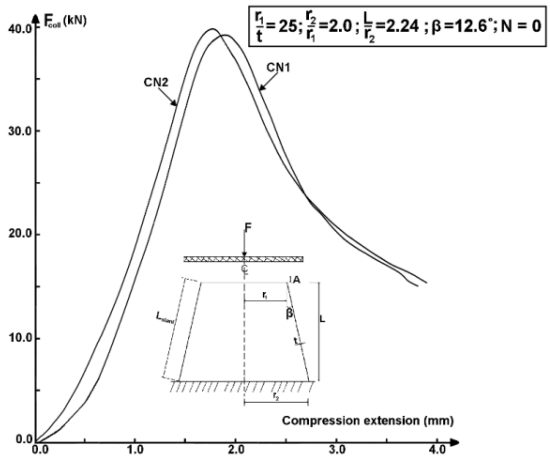

Figure 3: Plot of Axial Force Versus Compression Extension During Testing of Perfect Cones (CN1 and CN2)

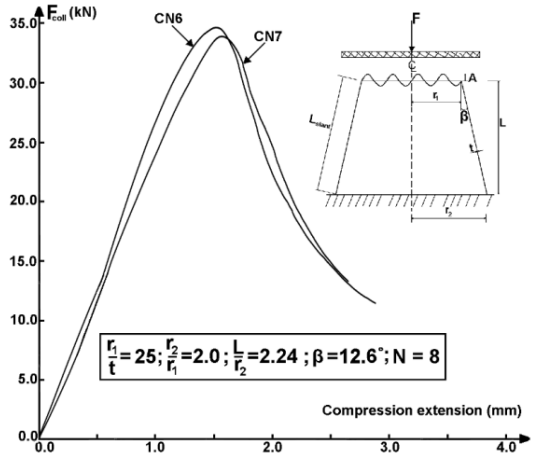

Figure 4: Plot of Axial Force Versus Compression Extension during Testing of Imperfect Cones (CN6 and CN7)

The ensuing results from the computation are given in column 5 of Table 3. From Table 3, it can be seen that there is a good agreement in the prediction of collapse load from both experiment and numerical simulation. The ratio of experimental load to numerical collapse load ranges from -4% to 9%, except for cones, CN5 and CN12, with 13% and 19%, respectively. All cones fail through bulging in the region where the compressed load is applied as exemplified for perfect and imperfect cones in Figure 5 (for cones with A/t = 0.28) and Figure 6 (for cones with A/t = 5.6). In addition, there is good visual agreement of both experimental and numerical deformed shape for the cones. However, the goodness of the comparison is seen to be strongly dependent on the contact interaction employed between the rigid plate and the deformed cone during the analysis. Results of benchmark of the contact interaction problem between rigid plate and the deformable cones through experimental test for cones with A/t = 0.28 and A/t = 5.6 reveals that the buckling load of the cone is strongly dependent on the imperfection amplitude. For cone with A/t = 0.28, the failure load is controlled by the contact interaction with set of top edge nodes (see Figure 5), while for cone with A/t = 5.6, the failure load is controlled by the contact interaction with set of N-point nodes (see Figure 6). However, it is not clear at what imperfection amplitude-to-thickness ratio does this change in contact interaction occurs. Hence, a need for more experimental studies in this area to establish the exact magnitude of A/t at which the changes occur.

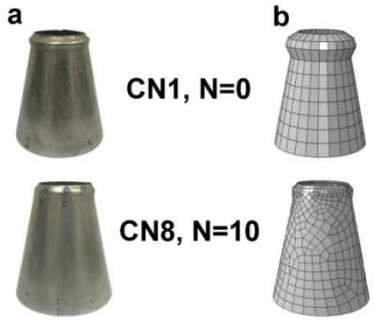

Figure 5: View of Deformed Perfect and Imperfect Cones with A/T = 0.28 (A) Experimental and (B) Numerical

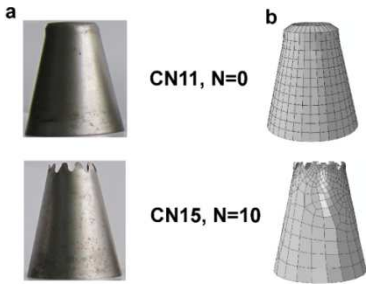

Figure 6: View of Deformed Perfect and Imperfect Cones With A/T = 5.6 (A) Experimental and (B) Numerical

CONCLUSIONS

Results of axial compressive test on fifteen conical model with non-uniform axial length was presented in this paper. Repeatability of experimental data was good. The results confirm the strong influence of non-uniform axial length on the load carrying capacity of the conical geometry considered. From the foregoing results, the following conclusions can be drawn: (i) the load carrying capacity of conical shell is strongly affected by the introduction of imperfect length. For instance, for cones having four sinusoidal wave on its compressed edge with imperfection amplitude-to-thickness ratio, A/t = 1.12, will lead to a large drop of about 28% of the load carrying capacity of the perfect cone, and (ii) the influence of contact problem on the load carrying capacity of axially compressed cone with non-uniform axial length is very significant and strongly dependent on the magnitude of imperfection amplitude-to-thickness ratio, A/t.

ACKNOWLEDGEMENTS

The authors will like to acknowledge the financial support received from Universiti Teknikal Malaysia Melaka (UTeM) and the Ministry of Education Malaysia under Fundamental Research Grant Scheme FRGS/2018/FTKMP-CARE/F00386.

REFERENCES

1. *Maali, M., Showkati, H., Fatemi, S.M.(2012). Investigation of the buckling behavior of conical shells under weld-induced imperfections. Thin-walled structures, 57, 13-24.*
2. *Goldfeld, Y., Sheinman, I., Baruch, M. (2003). Imperfection sensitivity of conical shells. AIAA Journal, 41, 517 – 524.*
3. *Ifayefunmi, O., Blachut, J.(2018). Imperfection sensitivity: A review of buckling behavior of cones, cylinders and domes. Journal of Pressure Vessel Technology Transaction of ASME, 140, 050801-1-050801-8.*
4. *Ifayefunmi, O. (2014). A survey of buckling of conical shells subjected to axial compression and external pressure. Journal of Engineering Science and Technology Review, 7, 182 - 189.*
5. *Błachut, J. (2013). Combined stability of geometrically imperfect conical shells. Thin-Walled Structures, 67, 121 - 128.*
6. *Błachut, J.(2012). Buckling of truncated cones with Localized imperfections. American Society of Mechanical Engineers, Pressure Vessels and Piping Division, Toronto, ON; Canada; 3, 3-11.*
7. *Khakimova, R., Warren, C.J., Zimmermann, R., Castro, S.G.P., Arbelo, M.A., Degenhardt, R. (2014). The single perturbation load approach applied to imperfection sensitive conical composite structures. Thin-Walled Structures, 84, 369-377.*
8. *Jabareen, M., Sheinman, I.(2006). Postbuckling analysis of geometrically imperfect conical shells. ASCE Journal of Engineering Mechanics, 132, 1326 - 1334.*
9. *Chikalthankar, S. B., Nandedkar, V. M., & Borde, S. V. (2013). Influence of Machining Parameters on Electric Discharge Machining of WPS Tool Steels–An Experimental Investigation. International Journal of Mechanical and Production Engineering Research and Development (IJMPERD), 3(5), 21-28.*
10. *Castro, S.G.P., Mittelstedt, C., Monteiro, F.A.C., Degenhardt, R., Ziegmann, G. (2015). Evaluation of non-linear buckling loads of geometrically imperfect composite cylinders and cones with the Ritz method. Composite Structures, 122, 284-299.*
11. *Goldfeld, Y. (2007). Imperfection sensitivity of laminated conical shells. International Journal of Solids and Structures, 44, 1221–1241.*
12. *Spagnoli, A. (2003). Koiter circles in the buckling of axially compressed conical shells. International Journal of Solids and Structures, 40, 6095-6109.*
13. *Chryssanthopoulos, M.K., Spagnoli, A. (1997). The influence of radial edge constraint on the stability of stiffened conical shells in compression. Thin-Walled Structures, 27, 147-163.*
14. *Castro, S.G.P., Mittelstedt, C., Monteiro, F.A.C., Arbelo, M.A, Ziegmann, G., Degenhardt, R. (2014). Linear buckling predictions of unstiffened laminated composite cylinders and cones under various loading and boundary conditions using semi-analytical models. Composite Structures, 118, 303-315.*
15. *Goldfeld, Y., Arbocz, J. (2004). Buckling of laminated conical shells given the variations of the stiffness coefficients. AIAA J. 42, 642–649.*
16. *Ilamparithi, A., Ponnusamy, S., & Selvaraj, A. (2014). Investigation On N-Formyl Piperidin-4-Ones As Corrosion Inhibitors For Carbon Steel In Acid Medium. Int. J. Appl. Nat. Sci., 3(2), 63-80.*
17. *Ifayefunmi, O., Kadmin, A. F., Chang, K.L., Aziz, A. (2018). Influence of boundary condition on the buckling of axially compressed cones and cylinders. International Journal of Mechanical Engineering and Technology, 9(4), 1106–1116.*
18. *Ali, D. (2013). Buckling of cracked conical frusta under axial compression. Research Journal of Recent Sciences, 2, 33-39.*

19. *Ifayefunmi, O. (2017). Plastic buckling of conical shell with non-continuous edge support. International Journal of Mechanical and Mechatronics Engineering, 17, 143–152.*
20. *Blachut, J.(2010). Buckling of axially compressed cylinders with imperfect length. Computers and Structures, 88, 365 – 374.*
21. *Blachut, J.(2015). Buckling of cylinders with imperfect length. Journal of pressure vessel technology, 137, 011203-1 – 011203-7.*
22. *Hibbitt, Karlsson, and Sorensen Inc. (2006). ABAQUS – Theory and Standard User's Manual Version 6.3. USA: Pawtucket, RI, 02860-4847.*
23. *George, J. P., & Pramod, V. R. (2014). An interpretive structural model (ISM) analysis approach in steel re rolling mills (SRRMS). International Journal of Research in Engineering & Technology (IMPACT: IJRET), 2(4), 161-174.*
24. *Błachut, J., Ifayefunmi, O.(2010). Buckling of Unstiffened Steel Cones Subjected to Axial Compression and External Pressure. Proceedings of the International Conference on Ocean, Offshore and Arctic Engineering (OMAE 2010), Vol. 2, OMAE2010-20518, pp. 385-398, ASME, NY, USA (ISBN: 978-0-7918-4910-1).*
25. *Błachut, J., Ifayefunmi, O., Corfa, M A.(2011). Collapse and Buckling of Conical Shells. Proceedings of the International Offshore (Ocean) and Polar Engineering Conference, ISOPE-2011 TPC-296, pp. 887-893, Cupertino, California, USA (ISBN 978-1-880653-96-8).*
26. *BS EN 10002-1. (2001). Tensile testing of Metallic Materials, Part (1), Method of test at ambient temperature. London, UK: British Standard Institute.*